Direct perovskite X-ray detector based on IGZO TFT backplane

Hao Liu, Dezhao Ma*, Xinhui Li*, Kuo Sun*, Hui Zhao*, Libin Liu*, Ling Shi*, Yinglong Huang**

* BOE Technology Group Co., Ltd, Beijing, China

Abstract

The direct flat panel detector, fabricated from perovskite materials with a peroxide thin film transistor (TFT) backplane, exhibited exceptional detection performance. With an active area of 1024 × 1024 pixels, each a 100 μm pitch, the detector boasts a spatial resolution of 4.3 lp/mm. The device employs an oxide TFT Gate Driver on Array (GOA) circuit for driving and is capable of capturing full-resolution images at 15 frames per second.

Author Keywords

IGZO TFT; GOA; Perovskite; Flat-Panel detector; Active matrix; Direct

1. Introduction

The TFT-based X-ray detector industry uses two distinct technological approaches: indirect and direct conversion methods. Indirect detectors, which utilize scintillators and PIN structures, struggle to achieve high spatial resolution due to limitations in filling factor and optical diffraction. Although detectors using amorphous selenium for direct conversion exhibit a very high intrinsic resolution, its limited absorption coefficient, high bias requirements, and poor temperature stability have hindered widespread adoption [1-3].

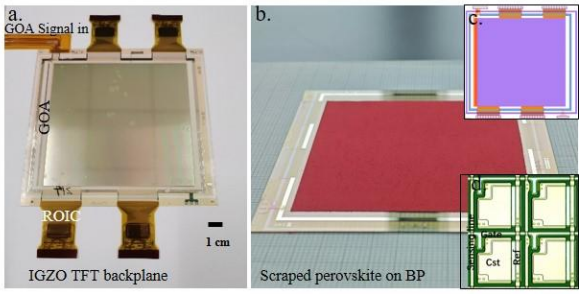

Figure 1. A 6 inch prototype perovskite direct conversion flat panel detector. a, IGZO TFT backplane driven by GOA circuit. b, Perovskite photoresponsive film prepared by solution method. c, IGZO TFT GOA-driven TFT backplane layout. d, The pixel structure of detector (Pitch 100 μm).

As research into perovskite materials progresses, their advantages in low-dose, high-speed imaging become increasingly apparent, due to their high X-ray absorption coefficient, long carrier lifetime, and low electric field drive requirements [4-6]. Compared to amorphous silicon, oxide TFTs offer higher electron mobility and lower leakage, enabling the transmission of more charge and faster response speeds, while generating less circuit noise [7,8].Consequently, flat panel detectors based on IGZO TFT backplane circuits hold great promise for realizing high-speed dynamic X-ray imaging. This paper aims to demonstrate the impressive characteristics of a 6 inch prototype perovskite direct conversion flat panel detector, as shown in Figure 1.

2. Detector discription

The direct conversion image detector comprises a layer of perovskite material deposited onto the substrate of an IGZO TFT array. The detector boasts a pixel resolution of 1024x1024, a pitch of 100 μm, and an effective sensing area of 10.24 cm x 10.24 cm. In contrast to indirect flat panel detectors, our direct conversion detector eliminates the P-I-N photodiode structure in the backplane, resulting in a geometric fill factor as high as 80%. In fact, due to this field effect, the effective fill factor is essentially 100% [9]. The pixel's stored capacitance (Cst) is 0.9 pF. Under 50 KV/1 mA radiation from an X-ray tube at a dose rate of 0.29mGy$_{air}$ s^{-1}, the detector can collect 9.8 pC of charge. The perovskite photoelectric conversion layer is prepared on the TFT substrate by scraping coating, with a thickness of 100 μm. The top electrode, consisting of Au/ITO, is deposited on the perovskite's upper surface using vacuum evaporation and magnetron sputtering.

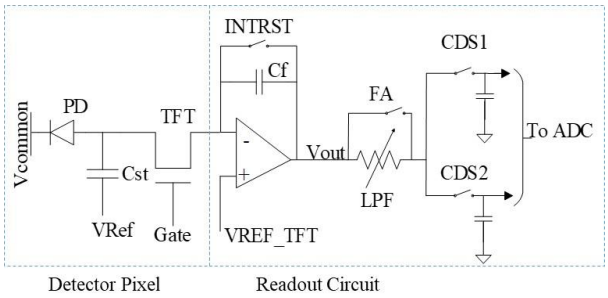

Figure 2. TFT Pixel and Readout Circuit.

PPS is used as an example that provides detailed information on the detector's configuration in Figure 2. Each pixel is equipped with a switching TFT that gates charge out to the integrating amplifier. V_{Gate} activates the readout TFT, enabling the transfer of photo-induced signals from a pixel to the external readout circuit. V_{common} and V_{REF_TFT}, voltages applied to the perovskite device, are set at the high voltage (18.8 V) and the low voltage (3.8 V), respectively. The perovskite device is illuminated through the transparent ITO and an ultra-thin Au electrode, resulting in the production of photogenerated charge carriers internally.

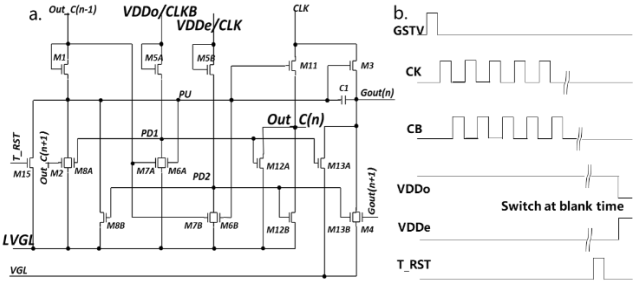

Figure 3. GOA Drive Circuit and Timing Diagram. .

ISSN 0097-996X/25/5602-1377-$1.00 © 2025

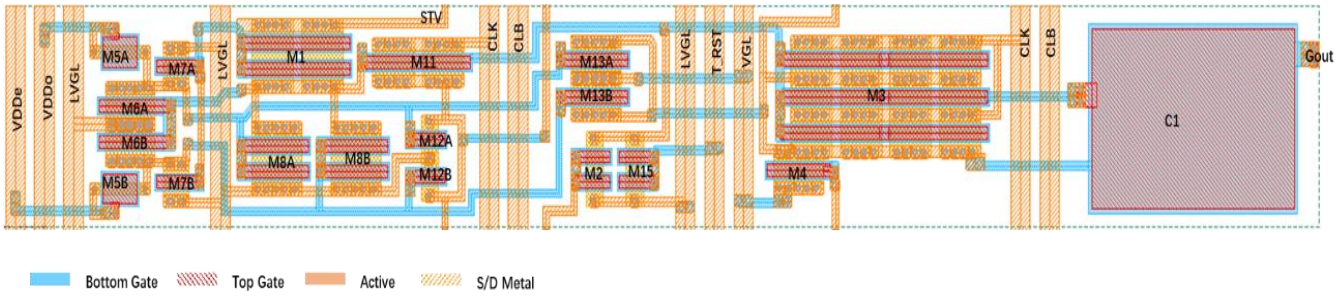

Figure 4. GOA circuit layout based on IGZO Dual Gate TFT.

Different from the traditional detector using gate IC for line scan drive, we proposed one 18T1C GOA circuit with high stability and reliability in this paper. All TFTs in GOA circuit are dual-gate TFT with top and bottom gate shorted. Additionally, the TFTs connected with PU (pull-up) points are designed as a parallel double-gate TFT structure, enhancing the potential retention ability of PU points. The GOA uses two sets of parallel design pull-up and pull-down control circuits that work alternately, and VDDo and VDDe are optionally designed for low-frequency pulse signals (e.g. 0.25Hz) to further improve the stability of TFT circuits while meeting the requirements of higher resolution, dynamic high refresh rates, and static low-frequency drivers. Considering the characteristics of IGZO TFT, we require a mobility greater than $10cm^2/V•S$ and a leakage current at 0V less than $10^{-15}A$. Due to the high electron mobility and low leakage current characteristics of IGZO TFT, the GOA demonstrated a stable signal output with Tr and Tf Values of 2.6 μs and 1.5 μs, respectively, as shown in Figure 5(b).

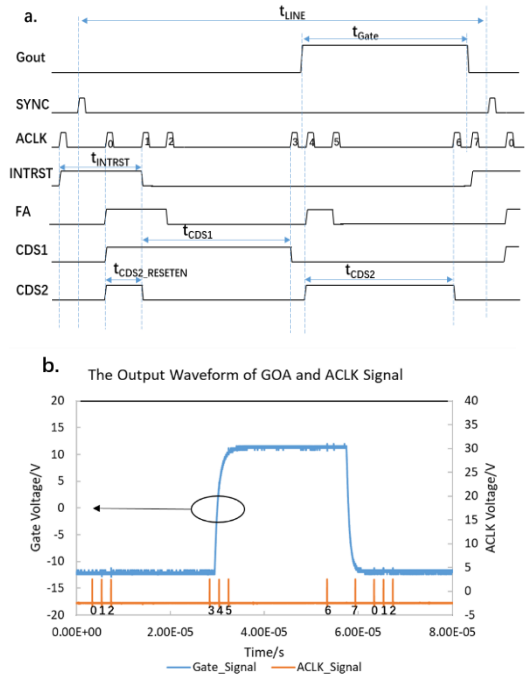

Figure 5. a, Control Signal Setting and Timing of Sampling Circuit. b, Actual Measurement of GOA and ACLK Signal Output Waveform.

The AD71200 ROIC (Readout Integrated Circuit) from Analog Devices is used to read out image charge from the TFT array, as depicted in Figure 1. By configuring the GOA driver and ROIC sampling timing by FPGA, the system is designed for full-resolution 15 Hz frame rate and 1024x1024 resolution sampling. Data is transmitted from ROIC to the host computer through a high-speed parallel link. AFE timing control is governed by the ACLK signal, with related switching activity occurring at the ACLK signal's rising edge.

ROIC operates in Pipeline mode, with sampling divided into three processes [9]. The first process (t_{INTRST} time) includes resetting the amplifier inverse (with feedback capacitor and CDS capacitor), the sensing line and its integrated capacitor. The second one (within t_{CDS1} time) is a sample of the background reset potential, and the last one (within t_{CDS2} time) is a sample of the pixel signal. The pixel signal is ultimately displayed as a voltage signal, with the output signal voltage satisfies the following equation:

$$V_{out} = V_{REF_{TFT}} - {}^{Q}/_{C_f} = V_{REF\_TFT} - {}^{S*D*A*t}/_{C_f} \qquad (1)$$

where V_{out} is the output voltage value of ADC, Q is the charge accumulated within Cst, Cf is the feedback capacitance value of the ROIC, S is the sensitivity of the perovskite material, D is the radiation dose rate, A is the effective filled area within a pixel, and t is the sampling time for one frame.

3. Result and Discussion

A 2mm thick stainless steel plate of 'B' was placed on top of the array and the X-ray image produced under a low dose. The X-ray tube is set at 50 kV /1 mA, with a corresponding irradiation dose rate of $0.29mGy_{air}\ s^{-1}$. The detector operates with a sampling frame rate of 15 Hz, resulting in an irradiation dose of $19\mu Gy_{air}$. The hollow letter 'B ' can be clearly detected, as shown in Figure 6. The black noise spots in the image are related to internal defects [10] in the perovskite and can be improved through subsequent film quality optimization.

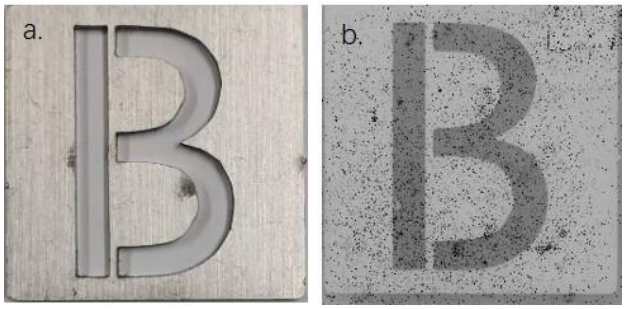

Figure 6. The "B" X-ray image of the hollow-out pattern obtained from a 256× 256 detector array (50 kV/1mA, $0.29mGy_{air}\ s^{-1}$, 15Hz frame rate sampling exposure for 67ms, producing a dose of 19 μGy_{air} and a common voltage of 18.8V).

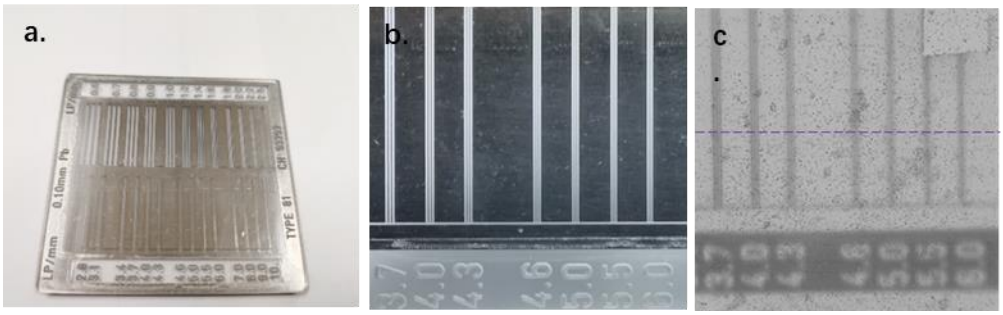

Figure 7. Radiograph of the resolution bar pattern illustrating high modulation.

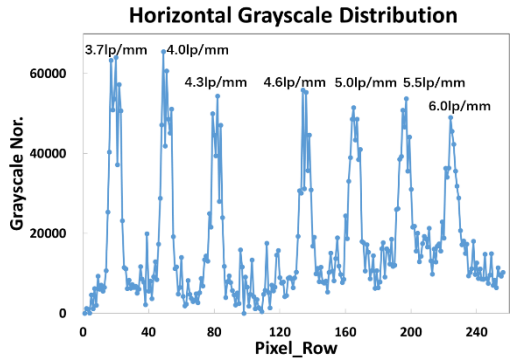

Figure 8. Gray scale curve of spatial resolution test.

Direct conversion primarily offers the potential for achieving extremely high image resolution. In comparison to high-resistance amorphous selenium, the currently higher dark current of perovskite still results in a certain degree of lateral crosstalk (lateral conduction process). Despite this, we conducted a preliminary measurement of the detector's X-ray irradiation imaging spatial resolution using a standard line pair card (type 81 CN93797). The line pair card was positioned at an angle of approximately 5° relative to the detector. The spatial resolution test results, shown in Figure 7, indicate that 4.3 lp can be identified under the limit state with R=20%, corresponding to a spatial resolution of 4.3 lp/mm.

4. Conclusion

The perovskite-based, direct conversion, oxide TFT flat panel detector proposed in this paper is well-suited for real-time imaging. Operating within the low dose range, it exhibits superior spatial resolution and excellent photo-response characteristics. When combined with GOA drive and flexible substrate integration, this device stands as a strong candidate for a new generation of flat panel detectors for low-dose dynamic imaging or 3D reconstruction.

In the imaging measurement of this detector, only the most basic background dark state signal was subtracted, and with no in-depth noise reduction or optimization algorithm processing was performed. In the future, we plan to adopt a more systematic approach to accurately evaluate the detector's performance and incorporate a digital image processing module into the software design, rather than limiting ourselves solely to data acquisition.

5. References

1. Shujie Tie, Siyin Dong, Ruihan Yuan, Bing Cai, Jianguo Zhu, Xiaojia Zheng. Halide perovskites for sensitive, stable and scalable X-ray detection and imaging. Chem Commun. 2023;
2. Zhe Du, Yongguang Hu, Noman Ali Buttar , et al. X-ray computed tomography for quality inspection of agricultural products: A review. Food Sci Nutr. 2019 Aug 23; 7(10):3146–60.
3. Tsung-Ter Kuo, Chien-Ming Wu, Isaac Chan, et al. Direct-Conversion X-Ray Detector with 50-µm High-Gain Pixel Amplifiers for Low-X-Ray-Dose Digital Mammography. J Med Biol Eng. 2015 Apr 3; 35(2):249–57.
4. Yimei Tan, Ge Mu, Menglu Chen, Xin Tang. X-ray Detectors Based on Halide Perovskite Materials. Coatings. 2023;
5. Shuang Zhou, Anders Brahme. Development of phase-contrast X-ray imaging techniques and potential medical applications. Phys Med. 2008 Sep 1; 24(3):129–48.
6. Haodi Wu, Yongshui Ge, Liduo Wang, Guangda Niu, Jiang Tang. Metal Halide Perovskites for X-Ray Detection and Imaging. 2021; 4(1):144–63.
7. Rikiya Takita, et al. Flexible Image Sensor Array Using IGZO TFT Backplane Technology for X-ray Detector. Proc Int Disp Workshop. 2020 Sep 18;
8. Chia-Ming Chang, Chia-Hsiu Tsai, Gengfu Zhou, Chun-Lin Chen, Ruei-Pei Chen. Flexible Image Sensor Array Using IGZO TFT Backplane Technology for X-ray Detector. SID Symp Dig Tech Pap. 2023;
9. Choquette M, Rougeot H, Martin JP, Jean-Pierre Martin, Laperriere L, Shukri Z, et al. Direct selenium x-ray detector for fluoroscopy, R&F, and radiography. 2000 Apr 25; 3977: 128–36.
10. Weicheng Pan, Bo Yang, et al. Hot-Pressed CsPbBr3 Quasi-Monocrystalline Film for Sensitive Direct X-ray Detection. Adv Mater. 2019 Sep 16; 31(44):1904405.